AFRL-ML-WP-TP-2007-502

NEW PHENOMENA IN DYE-DOPED LIQUID CRYSTALS: BLACK HOLE EFFECT AND SWITCHABLE REVERSED DIFFRACTION (PREPRINT)

D.R. Evans, G. Cook, M.A. Saleh, J.L. Carns, S. Serak, and N. Tabiryan

Hardened Materials Branch
Survivability and Sensor Materials Division

JANUARY 2006

AIR FORCE RESEARCH LABORATORY
MATERIALS AND MANUFACTURING DIRECTORATE
WRIGHT-PATTERSON AIR FORCE BASE, OH 45433-7750
AIR FORCE MATERIEL COMMAND
UNITED STATES AIR FORCE

NOTICE AND SIGNATURE PAGE

Using Government drawings, specifications, or other data included in this document for any purpose other than Government procurement does not in any way obligate the U.S. Government. The fact that the Government formulated or supplied the drawings, specifications, or other data does not license the holder or any other person or corporation; or convey any rights or permission to manufacture, use, or sell any patented invention that may relate to them.

This report was cleared for public release by the Air Force Research Laboratory Wright Site (AFRL/WS) Public Affairs Office and is available to the general public, including foreign nationals. Copies may be obtained from the Defense Technical Information Center (DTIC) (http://www.dtic.mil).

AFRL-ML-WP-TP-2007-502 HAS BEEN REVIEWED AND IS APPROVED FOR PUBLICATION IN ACCORDANCE WITH ASSIGNED DISTRIBUTION STATEMENT.

*//Signature//

DEAN R. EVANS, Ph.D.
Agile Filters Project
Exploratory Development
Hardened Materials Branch

//Signature//

MARK S. FORTE, Acting Chief
Hardened Materials Branch
Survivability and Sensor Materials Division

//Signature//

TIM J. SCHUMACHER, Chief
Survivability and Sensor Materials Division

This report is published in the interest of scientific and technical information exchange, and its publication does not constitute the Government's approval or disapproval of its ideas or findings.

*Disseminated copies will show "//Signature//" stamped or typed above the signature blocks.

REPORT DOCUMENTATION PAGE

Form Approved
OMB No. 0704-0188

1. REPORT DATE *(DD-MM-YY)*	2. REPORT TYPE	3. DATES COVERED *(From - To)*
January 2006	Journal Article Preprint	

4. TITLE AND SUBTITLE

NEW PHENOMENA IN DYE-DOPED LIQUID CRYSTALS: BLACK HOLE EFFECT AND SWITCHABLE REVERSED DIFFRACTION (PREPRINT)

5a. CONTRACT NUMBER
In-house

5b. GRANT NUMBER

5c. PROGRAM ELEMENT NUMBER
62102F

6. AUTHOR(S)

D.R. Evans (AFRL/MLPJ)
G. Cook (Universal Technology Corporation)
M.A. Saleh (UES, Inc.)
J.L Carns (General Dynamics Information Technology, Inc.)
S. Serak and N. Tabiryan (BEAM Engineering for Advanced Measurements Co.)

5d. PROJECT NUMBER
4348

5e. TASK NUMBER
RG

5f. WORK UNIT NUMBER
M08R1000

7. PERFORMING ORGANIZATION NAME(S) AND ADDRESS(ES)

Hardened Materials Branch (AFRL/MLPJ)
Survivability and Sensor Materials Division
Materials and Manufacturing Directorate
Wright-Patterson Air Force Base, OH 45433-7750
Air Force Materiel Command, United States Air Force

Universal Technology Corporation
1270 North Fairfield Road
Dayton, OH 45432

UES, Inc.
4401 Dayton-Xenia Road,
Dayton, OH 45432

General Dynamics Information Technology, Inc.
5100 Springfield Pike, Suite 509
Dayton, OH 45431

BEAM Engineering for Advanced Measurements Co.
809 South Orlando Avenue, Suite I
Winter Park, FL 32789

8. PERFORMING ORGANIZATION REPORT NUMBER
AFRL-ML-WP-TP-2007-502

9. SPONSORING/MONITORING AGENCY NAME(S) AND ADDRESS(ES)

Air Force Research Laboratory
Materials and Manufacturing Directorate
Wright-Patterson Air Force Base, OH 45433-7750
Air Force Materiel Command
United States Air Force

10. SPONSORING/MONITORING AGENCY ACRONYM(S)
AFRL/MLPJ

11. SPONSORING/MONITORING AGENCY REPORT NUMBER(S)
AFRL-ML-WP-TP-2007-502

12. DISTRIBUTION/AVAILABILITY STATEMENT
Approved for public release; distribution unlimited.

13. SUPPLEMENTARY NOTES
Journal article submitted to Molecular Crystals and Liquid Crystal. The U.S. Government is joint author of this work and has the right to use, modify, reproduce, release, perform, display, or disclose the work. PAO Case Number: AFRL/WS 06-0320, 07 Feb 2006.

14. ABSTRACT

A nonlinear extinction of transmitted light is observed in liquid crystal cells with large concentrations of anthraquinone dye. Two distinctr mechanisms are responsible for this effect when exposed to low and high intensity light, respectively. At low intensities, critical opalescence, micro-scatter, and an increase in linear absorption occur; whereas high intensities result in scattering from photo-induced micro-bubbles.

15. SUBJECT TERMS
Liquid Crystal, Anthraquinone Dye, Critical Opalescence, Micro-Domains, Bubbles, Marangoni Effect

16. SECURITY CLASSIFICATION OF:			17. LIMITATION OF ABSTRACT:	18. NUMBER OF PAGES	19a. NAME OF RESPONSIBLE PERSON (Monitor)
a. REPORT	b. ABSTRACT	c. THIS PAGE			Dean R. Evans
Unclassified	Unclassified	Unclassified	SAR	24	19b. TELEPHONE NUMBER *(Include Area Code)* N/A

Standard Form 298 (Rev. 8-98)
Prescribed by ANSI Std. Z39-18

New Phenomena in Dye-Doped Liquid Crystals: Black Hole Effect and Switchable Reversed Diffraction

D. R. Evans[1], G. Cook[1,2], M. A. Saleh[1,3], J. L. Carns[1,4], S. Serak[5], and N. Tabiryan[5]

[1]*Air Force Research Laboratory, Materials and Manufacturing Directorate*
Wright-Patterson Air Force Base, OH 45433
[2]*Universal Technology Corporation, 1270 N. Fairfield Road, Dayton, Ohio 45432*
[3]*UES, Inc., 4401 Dayton-Xenia Road, Dayton, Ohio 45432*
[4]*Anteon Corporation, 5100 Springfield Pike Suite 509, Dayton, Ohio 45431*
[5]*BEAM Engineering for Advanced Measurements Co.*
809 South Orlando Ave., Suite I, Winter Park, Florida 32789

Abstract

A nonlinear extinction of transmitted light is observed in liquid crystal cells with large concentrations of anthraquinone dye. Two distinct mechanisms are responsible for this effect when exposed to low and high intensity light, respectively. At low intensities, critical opalescence, micro-scatter, and an increase in linear absorption occur; whereas high intensities result in scattering from photo-induced micro-bubbles.

Keywords: Liquid Crystals, Anthraquinone Dye, Critical Opalescence, Micro-domains, Bubbles, Marangoni Effect

Introduction

One of the more important developments in nonlinear optics of liquid crystals (LCs), following the discovery of the orientational mechanism of optical nonlinearity [1-3], is the comprehension that the nonlinear refraction of LCs could be enhanced by one to two orders of magnitude due to the addition of certain dyes. These enhancements of the optical nonlinearities have been observed with dye concentrations as low as 0.1 wt.% [4-6]. The presence of dyes in LCs has been shown to be an effective means of increasing the nonlinear extinction of radiation due to physical processes such as absorption or scattering [7-9].

Large concentrations of dye in LCs have not been investigated to the same level as weakly doped materials. In the present paper we show that increasing the dye concentration of anthraquinone (AQ) doped LCs to saturable levels results in new intricate processes of light extinction and scattering. The physical mechanisms responsible for these processes have been determined to be rather different for low and high intensities of laser light. At low intensities, the transmitted light appears to vanish under certain conditions due to critical opalescence, formation of micro-domains and enhanced absorption, and has been dubbed the "Black Hole" effect. Above a critical pump intensity, the light is abruptly back-scattered due to the generation of micro-bubbles invoking the term "Switchable Reversed Diffraction" (SRD).

Material and Experimental Description

LC cells consisting of 4-pentyl-4'-cyanobiphenyl (5CB), with thicknesses of 30 μm, 50 μm, and 80 μm, were doped with various concentrations of 1,8-dihydroxy,4,5-diamino,2,7-diisopentyl-anthraquinone (AQ) dye ranging from 0.3 wt. % to 2.0 wt. %. The molecular structures of both the host LC (5CB) and the AQ dye are shown in Fig. 1.

The glass substrates were covered with 0.5 wt.% solution of poly(vinylalcohol) (PVA) in distilled water and spin-coated for 30 s at 4000 rpm. The PVA films dried at 80°C for 20 min. and were then rubbed anti-parallel with a cloth to yield a planar alignment. The 30 μm thick LC cells were doped with various concentrations (0.3, 0.6, 0.75, 0.85, 1.0, 1.2, and 1.5 wt. %) of AQ dye, which were used to determine the influence of the linear absorption on the black hole effect. The 50 μm thick cells, doped with either 1.2 wt.% or 2.0 wt. % AQ dye, were used for the investigation of the scattering effects, micro-domain and critical opalescence, associated with the black hole effect. The 80 μm thick cell contained 2.0 wt. % AQ dye and was used for the study of the SRD effect.

Several different experiments were conducted for this study. Absorption spectroscopy was used to compare the effects of concentration on the linear absorption of the nematic and isotropic phases. The dynamics of both the black hole and SRD effects were characterized using either an unpolarized continuous wave (CW) 633 nm He-Ne laser (Coherent 31-2082-000) or a linearly polarized CW 532 nm laser (Coherent Verdi), respectively. Near-field images of these effects were observed with a CCD camera; the experimental arrangement used for collecting these images is shown in Fig. 2a. A Hitachi KP20B CCD was used for the investigation of the black hole effect, whereas a Sony DC-77RR CCD was used for the investigation of the SRD. Far-field images were observed in a similar manner where the light transmitted through the LC cell onto a screen; without the use of the white light source, 10X microscope objective, notch filter, and CCD camera as shown in Fig. 2a. To quantify the SRD effect in the thick cell, both transmission and reflection measurements were conducted using an integrating sphere, where the cell was placed at normal incidence in the focal plane as shown in Fig. 2(b,c). Because of the thickness and large absorption coefficient of the cell used for the SRD effect studies, 532 nm was selected in order to reduce the absorbance. The hysteresis curve of the divergence angle as a function of input power, as related to the SRD effect, was measured in the same cell using a 35 mm focal length lens (f/47) to focus the laser light onto the sample. The transmitted beam was viewed on a screen placed 36 mm behind the LC cell. Except where specified, the focusing conditions used were f/27 and f/14 for the black hole and SRD measurements, respectively.

Results and Discussion

Part 1 – Black Hole Effect

The black hole effect is described in Fig. 3, where the laser beam exiting of the LC cell is shown for various positions of the cell with respect to the focal plane. At weak intensities (< 1 W/cm^2) light is transmitted through the cell without undergoing nonlinear effects (Fig. 3a,e). Increasing the intensity of light on the LC cell results in local heating, which changes the LC/dye mixture from a nematic to an isotropic phase. At higher intensities (> 10 kW/cm^2), when the cell is placed at the beam waist, self phase modulation occurs, as shown is Fig. 3c. This is apparent by the typical nonlinear phase modulation pattern observed in the far-field [1-3]. In between these positions at an intermediate focal position, (Fig. 3b,d), where the incident intensity is ~10 W/cm^2, the transmitted beam disappears. Although it is not shown in Fig. 3 at intermediate positions (between positions A and B and positions D and E) a single ring forms, which we believe is due to the threshold of self-focusing giving rise to an on-axis intensity spike in the near field and the Fourier transform of this in the far field (a single ring). Upon recollimation,

the beam quality is restored indicating the average phase profile is not significantly distorted. The transmission of the 2.0 wt% AQ doped LC cell as a function of distance from focus for different incident powers is shown in Fig. 4; the cell was translated at 450 μm/s. At low power levels the transmission reaches a minimum at the focal plane of the lens and decreases with increasing incident power. Starting from around 4 mW, the transmission in the focus increases with increasing power. The effect of a decreasing transmission at such higher power values is further observed in the vicinity, however, at a distance from the focus.

There are several mechanisms considered to be associated with the black hole effect: micro-domain scatter, critical opalescence, and enhanced absorption. Figure 5 shows the effect of the micro-domain scatter, where heat generated from the strong absorption of the dye drives the LC molecules to phase transition point. A laser beam of 14.4 mW power was focused onto a 50 μm cell using an f/80 focusing optics in these tests. In order to observe the domain structure, the LC cell was placed between crossed-polarizers on a microscope stage such that the LC director was at 45° with respect to the polarizers in order to block the laser light after the cell. The near-field images were viewed using a 10X microscope objective and a CCD camera. Immediately after the laser beam was removed, a large density of micro-domains was observed. On the order of 100 ms after the laser beam was switched off, there was a reduction in the density of these micro-domains; several seconds later the micro-domains vanished. Although the role of the dye in this process is believed to be a source of heat generation, it is not excluded that the dye molecules could form aggregates that would split the LC orientation into small domains as well.

In addition to the micro-domains, critical opalescence also contributes to the scattering effect when the nematic and isotropic phases approach a critical density. Figure 6 shows the difference between the micro-domain (Fig. 6a) and critical opalescence (Fig. 6b) scattering mechanisms, where the physical appearance of these two mechanisms is quite distinct when observed in the near-field. A direct observation of critical opalescence in the AQ dye doped LC cell, while scanning the sample across the laser beam, shows a milky scattering structure as shown in Fig. 6b.

Another contributing mechanism to the black hole effect is the enhanced absorption experienced in the isotropic phase. When the LCs are heated into the isotropic phase by the incident laser beam; the linear absorption of the AQ/LC mixture in the isotropic phase increases. When the concentration of dye is above 0.3 wt.%, the absorption in the isotropic phase becomes significantly greater than that of the nematic phase. Figures 7(a,b) show the linear absorption spectra for two different concentrations of AQ dye in the 30 μm thick cells (0.3 and 1.2 wt.%); the absorption in the two phases is nearly equal at 0.3 wt.% dye and almost a factor of two different for the cell with 1.2 wt.% dye. In Fig. 7c, the absorption coefficients as a function of dye concentration for a laser beam polarized parallel and perpendicular to the orientation of the LCs, and the absorption coefficients measured in the isotropic phase α_{iso} and $<\alpha>$ are shown for the wavelength 633 nm. The absorption coefficients are defined for the intensity of the beam: $I_{out} = I_{in}\exp(-\alpha L)$ where I_{in} and I_{out} are the intensity values at the input and output of the LC cell, respectively. It is interesting to note that the measured value of the absorption coefficient in the isotropic phase is larger than the expected average value that is calculated by individual measurements of the absorption coefficients for laser beam

polarization parallel and perpendicular to the orientation direction of the LC $<\alpha> = (\alpha_{||} + 2\alpha_{\perp})/3$. This discrepancy increases with greater dye concentrations. This is a clear indication that a large dye concentration triggers complex processes in the material, such as formation of dye aggregates with a temperature dependent "aggregation number," as well as diffusion. It would be speculative to make more specific statements without detailed further research of this phenomenon.

Part 2 - Switchable Reversed Diffraction

The effect of relatively high intensities on a LC cell with a large concentration of dye, 2.0 wt.% AQ, is examined in this part of the work. A CW 532 nm laser is used rather than the He-Ne because the absorption is weaker at this wavelength allowing for a more detailed analysis of the transmitted and reflected beams with less of a loss due to the strong absorbance. The same effect is observed in the red, but with a lower switching threshold intensity because of the larger linear absorption in that spectral region (see Fig. 7).

At relatively high intensities (up to 25 kW/cm^2), when the cell is placed at the beam waist, the transmitted light through the LC cell forms concentric ring patterns, where the inner rings are fine and the outer rings are coarse, shown in Fig. 8a at position S_2. This ring pattern is characteristic of self-focusing due to thermal indexing, which is the change in the index of refraction due to the inhomogeneous heating of the material, as is also the case in Fig. 3c. The inhomogeneous heating is due to the Gaussian profile of the laser beam. The Fresnel reflection from the cell counter-propagates along the incident beam and can be seen around the entrance hole of the screen at position S_1. The transmission increases linearly with incident power, although the transmitted intensity decreases because the ring pattern increases in diameter with increasing power.

As the incident power is increased to a threshold power ~18 mW (~25 kW/cm^2), an apparently instantaneous switching effect occurs, where a significant amount of the transmitted light suddenly reverses direction becoming counter-propagating (SRD). This effect is shown in Fig. 8b, where the transmitted beam at position S_2 is relatively weak and the backward diffracted beam at position S_1 is significantly greater in intensity. Unlike the transmitted ring pattern at lower intensities, the reversed diffracted rings are of equal space and thickness. It was observed that the switching occurs due to the formation of a gaseous micro-bubble which acts as a micro-mirror as seen in Fig. 9c. Even though the LCs are degassed in a vacuum chamber before making the LC cells, it may be possible that some air stays in them forming the micro-bubbles when enough heat is generated. For comparison the LCs in the nematic and isotropic states and the corresponding transmission patterns are shown in Figs. 9a and 9b, respectively. Because of the spherical nature of the gas bubble, the reversed diffraction direction is independent of the angle of the incident beam. Even with the cell set at a 70° tilt with respect to the incident beam, the reversed diffracted beam counter-propagates along the incident beam, rather than in the direction of the Fresnel reflection. This is only true as long as the micro-bubble generated is smaller than the thickness of the cell. Micro-bubbles generated with a power level significantly greater than threshold do not allow for pure counter-propagating beams. The micro-bubbles increase in size with power, when their diameter is on the order of the thickness of the LC cell they are distorted by the cell boundaries.

In order to quantify the amount of transmitted and reversed diffracted light, transmission and reflection measurements were conducted using an integrating sphere. The light was focused onto the cell while it was mounted at the entrance port of the integrating sphere. The transmitted light was collected in the integrating sphere and the results are shown in Fig. 10a. For input powers up to 10 mW (~14 kW/cm^2) the transmission is linear. The transmission becomes nonlinear over a power range of 10 - ~18 mW (~14 – ~25 kW/cm^2), indicating that the absorption is increasing. In this power range the LCs are in the isotropic state; the increased absorption corresponds with the results seen in Fig. 7. At ~25 kW/cm^2 there is a sudden increase in transmitted power, although the overall intensity is reduced as seen in Fig. 8b. The transmitted light increases after the formation of the micro-bubble, because a small region of highly absorbing dye is replaced with a non-absorbing gas.

For reflection measurements, the light was focused through the integrating sphere onto the cell while it was mounted at the exit port of the integrating sphere. The Fresnel reflection was reflected back through the entrance port in order to minimize the detection of scattered light inside the integrating sphere. A bare window was used as a reference, which shows only a small amount of scatter over the power range used. Replacing the bare window with the LC cell, a sudden increase in reflected power is seen at the same power threshold as the increased transmission occurs.

To verify that the intensity actually decreases although the transmitted power has been shown to increase, the hysteresis of the scattering angle (divergence) of the transmitted light is determined as a function of input power as shown in Fig. 11. When increasing the power up to the threshold of reversed diffraction (18-20 mW), the angle of divergence gradually increases from 0.25 rad to 0.79 rad. When the micro-bubble forms at the threshold power, in this case ~18.5 mW, the transmitted beam divergence suddenly jumps from 0.79 to 2.25 rad. Once switched, the beam divergence remains at 2.25 rad down to power levels (5.8 mW, 8 kW/cm^2) that are unable to sustain the micro-bubbles. Once a micro-bubble is formed, it remains in the laser beam, even at a fraction of the threshold power required for its formation. When the laser intensity (i.e. generated surface tension) is too weak to hold the micro-bubble (< 5.8 mW) in the path of the focused beam, the bubble floats away and the transmitted beam returns to 0.25 rad divergence. The reason for the trapping of the bubble in the laser beam is related to the Marangoni Effect [10]. The gradient of heat generated in the laser beam yields a surface tension gradient. The liquid flows from regions with low surface tension to regions with a higher surface tension. For volume conservation, the bubble moves the opposite way (to fill the fluid void). When the heat generated by absorption is inadequate to generate the required surface tension, the bubble breaks loose and floats away.

Conclusions

Two different effects have been observed in LCs with large concentrations of AQ dye depending on the incident intensity. At low intensities, the effect in which the light disappears at the output of the LC cell has been referred to as the black hole effect. This effect is due to micro-domain scatter, critical opalescence, and enhanced absorption in the isotropic phase. At high intensities, SRD occurs when photo-induced micro-bubbles reflect (or diffract) light in a counter-propagating direction, regardless of the angle of incidence of the laser beam. A highly concentrated dye doped LC cell allows for the

ability to manipulate light over a large range of intensities using different physical mechanisms in a single cell.

Acknowledgements

The authors would like to thank Kevin Cissner, Roger Becker, and Richard Sutherland for useful discussion and David Zelmon for the use of an integrating sphere.

References

[1] N. V. Tabiryan, B. Ya. Zel'dovich, A. V. Sukhov, *Special Issue of Mol. Cryst. Liq. Cryst.,* **136** (1), 1, (1986).

[2] I. C. Khoo, *Liquid crystals: physical properties and nonlinear optical phenomena.* Wiley Interscience: New York, (1994).

[3] F. Simoni, *Nonlinear optical properties of liquid crystals and polymer liquid crystals.* World Scientific: Singapore, (1997).

[4] I. Janossy, A.D. Lloyd, B.S. Wherrett, *Mol. Cryst., Liquid Cryst.,* **179,** 1, (1990).

[5] I. C. Khoo, P. H. Chen, M. Y. Shih, A. Shishido, S. Slussarenko, *Mol. Cryst. Liq. Cryst.,* **358**, 1, (2001).

[6] L. Marrucci, *Liquid Crystals Today,* **11** (3), 6, (2002).

[7] N. V. Tabiryan, U. A. Hrozhyk, H. L. Margaryan, M. J. Mora, S. R. Nersisyan, S. V. Serak, *Mat. Res. Soc. Symp. Proc.*, **709**, 91, (2002).

[8] N. V. Tabiryan, S. V. Serak, V. A. Grozhik, *J. Opt. Soc. Am. B,* **20** (3), 1, (2003).

[9] N. V. Tabiryan, S. Nersisyan, *Opt. Eng.,* **41**, 2876, (2002).

[10] M. G. Velarde and R. K. Zeytourian (Eds.), *Interfacial Phenomena and the Marangoni Effect.* Springer: New York (2002).

Figure Captions

Fig. 1 The structural formula and modeling of the molecules of the component materials: a) nematic liquid crystal 4-pentyl-4'-cyanobiphenyl (5CB); b) anthraquinone dye: 1,8-dihydroxy,4,5-diamino,2,7-diisopentyl-anthraquinone.

Fig. 2 The experimental arrangements for near-field imaging (a) and integrated power measurements (b,c). The arrangement in schematic (a) consists of a lens (L), a liquid crystal cell (LC), a white light source (W), a microscope objective (O), a notch filter (F), and a CCD camera (C). The arrangement in schematics (b,c) consist of a lens (L), a liquid crystal cell (LC), an integrating sphere (IS), and an external power detector (P). Arrangement (b) is used for transmission measurements, where a blank cover (BL) is on the exit port for case. Arrangement (c) is used for reflection measurements where an aperture (AP) is used on the entrance port.

Fig. 3 Far-field image of the transmitted light: a,e) Normal transmission, b,d) black hole effect, and c) self phase modulation.

Fig. 4 Transmission of the 2 wt% AQ doped LC cell as a function of distance from focus for different powers of an unpolarized 633 nm laser beam. The powers used were (a) 0.5 mW, (b) 0.7 mW, (c) 1.7 mW, (d) 3.8 mW, (e) 5.2 mW, and (f) 9.3 mW.

Fig. 5 Near-field images of the micro-domain structure as a function of time. The times listed correspond to the duration of time past since the laser beam was removed.

Fig. 6 (a) Formation of micro-domain structure immediately after switching off the He-Ne laser beam. (b) Direct observation of critical opalescence when scanning the red laser beam across the sample.

Fig. 7 Unpolarized absorption spectra of the dye doped LC cells as a function of concentration, a) 0.3 wt. %, b) 1.2 wt. %. The solid curves are the spectra measured in the isotropic phase and the dotted curves are the spectra measured in the nematic phase. Cc) Absorption coefficient (α) as a function of dye concentration for a laser beam polarized parallel ($\alpha_{||}$) and perpendicular ($\alpha_{\perp}$) to the orientation of LCs. α_{iso} and $<\alpha>$ are the measured absorption coefficients in the isotropic phase.

Fig. 8 Far-field images are the transmitted and reverse diffracted light from the dye doped LC cell. The experimental arrangement consists of a lens (L), a liquid crystal cell (LC), and screens (S_1 and S_2), where the incident laser beam entered through the screen at S_1.

Fig. 9 Diagrams of the scattering effects observed as a function of input intensity and the corresponding images of the liquid crystal in the (a) nematic state, (b) isotropic state, and (c) gaseous state (presence of a micro-bubble).

Fig. 10 Integrated transmitted (a) and reflected (b) powers as a function of input power (squares). The inset in trace (a) is an enlargement of the weaker input powers (0 – 20 mW). The open circles in trace (b) are the reflected light values from a bare window.

Fig. 11 Hysteresis of the scattering angle of the transmitted light as a function of input power. The inset is a schematic of the experimental arrangement.

Fig. 1

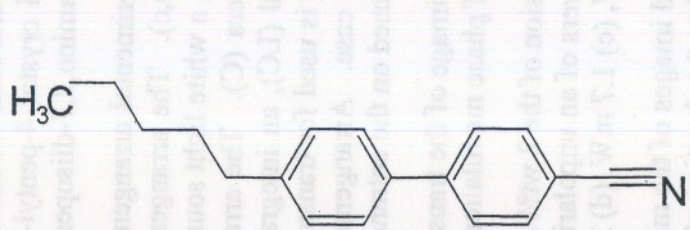

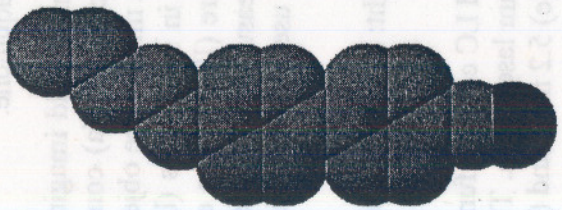

a

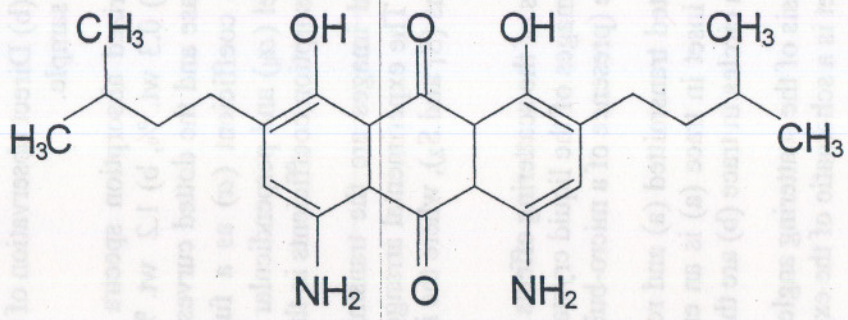

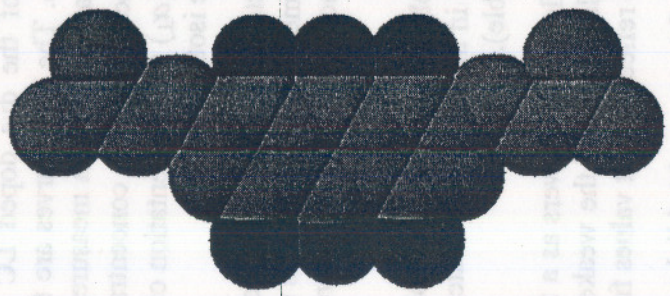

b

Fig. 2

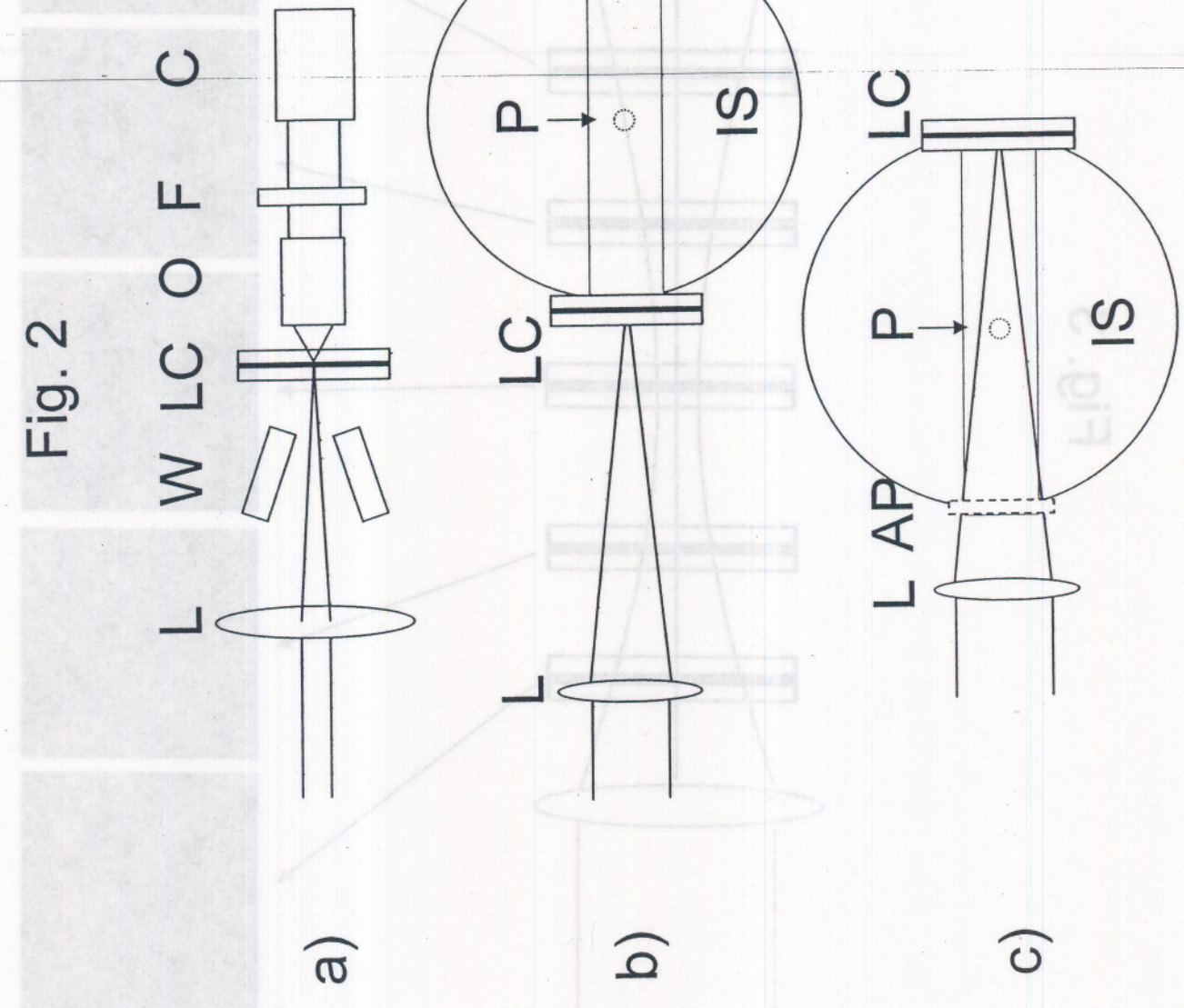

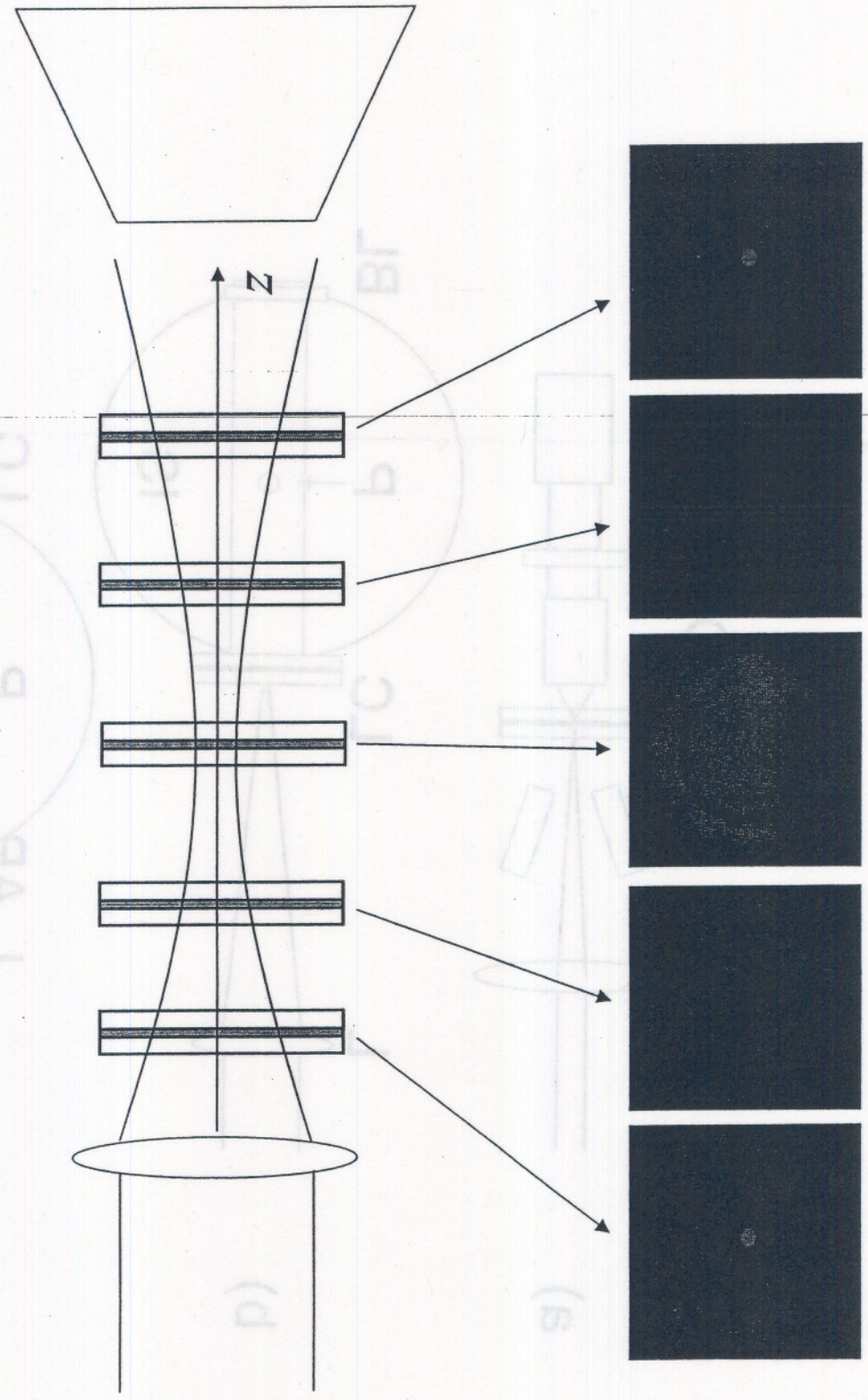

Fig. 3

Fig. 4

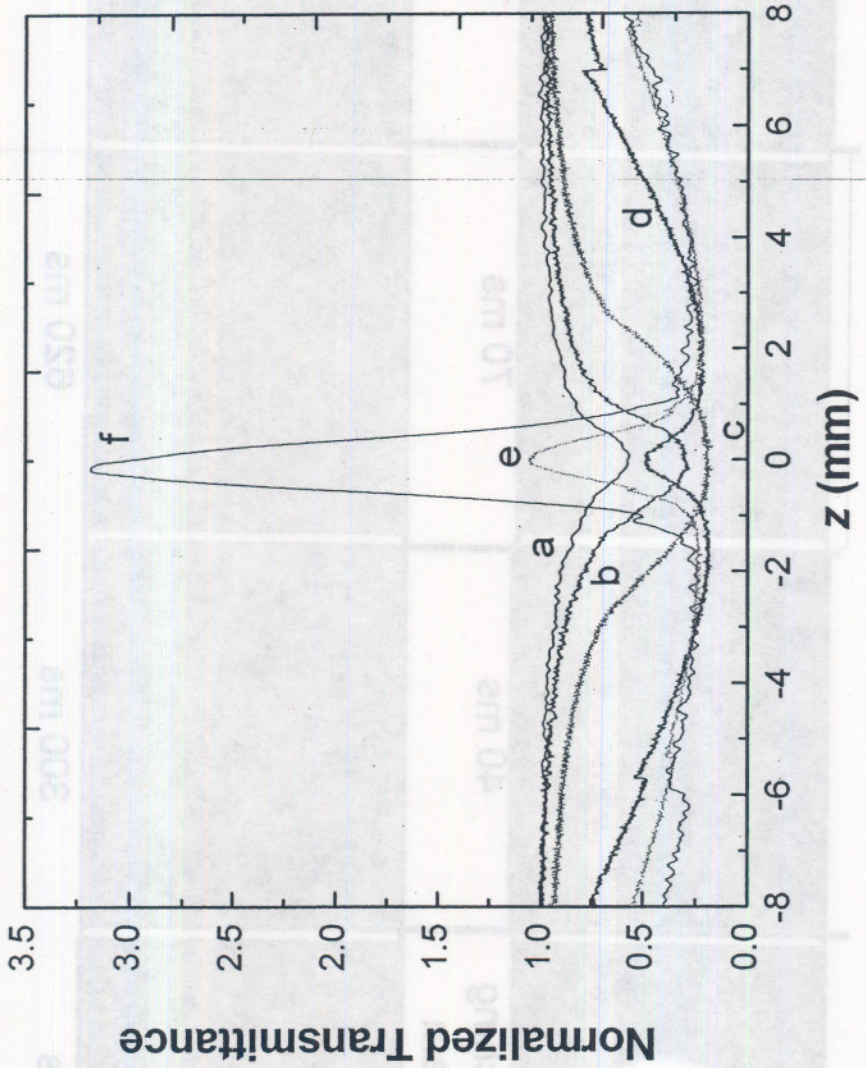
Normalized Transmittance
z (mm)
3.5
3.0
2.5
2.0
1.5
1.0
0.5
0.0
-8
-6
-4
-2
0
2
4
6
8
a
b
c
d
e
f

Fig. 5

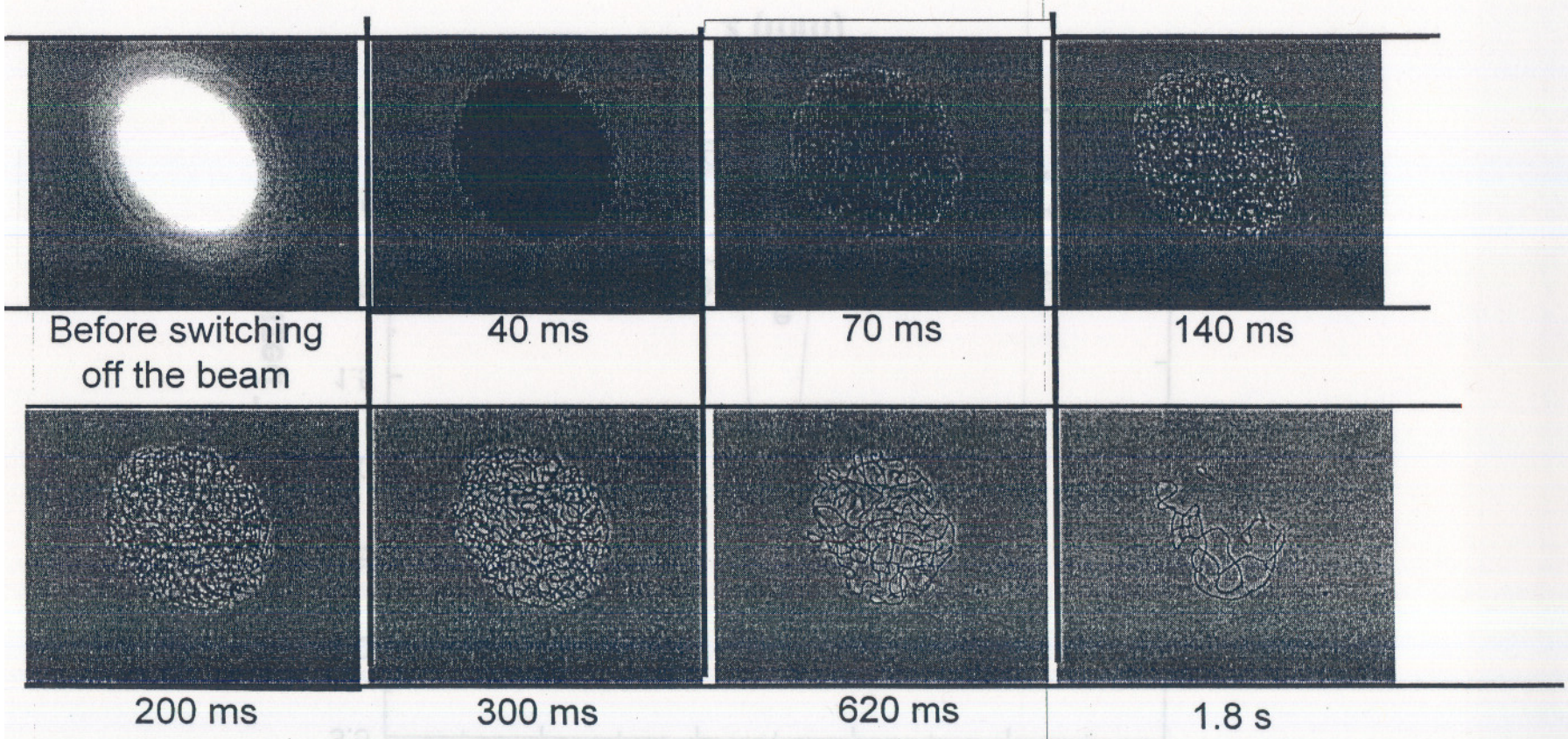
Before switching off the beam
40 ms
70 ms
140 ms
200 ms
300 ms
620 ms
1.8 s

Fig. 6

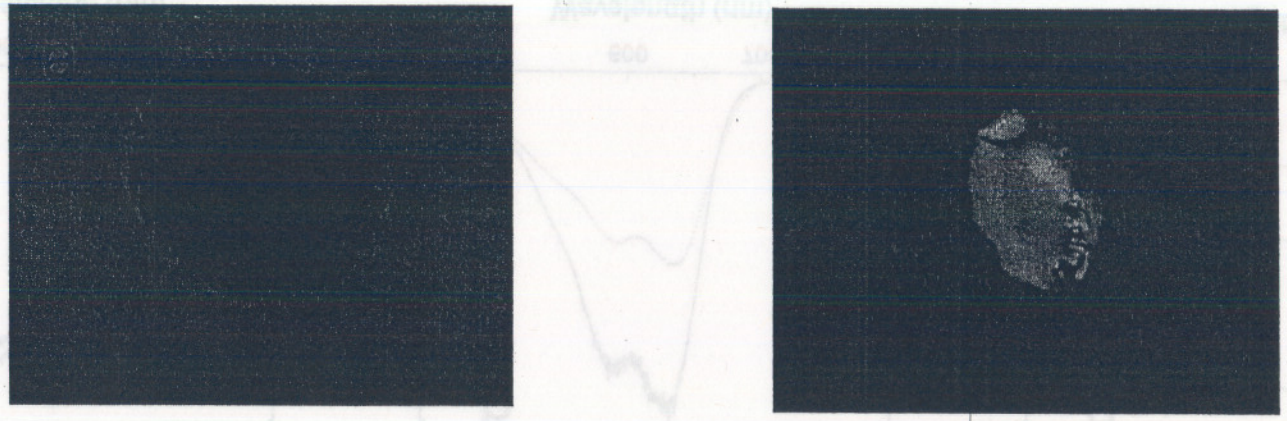

Fig. 7

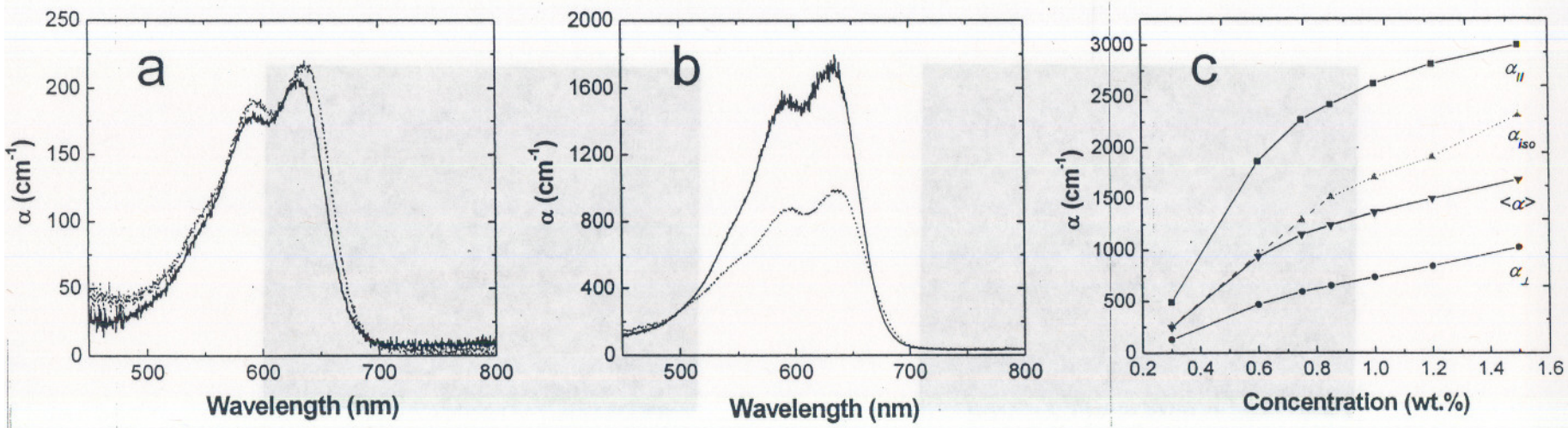

Fig. 8

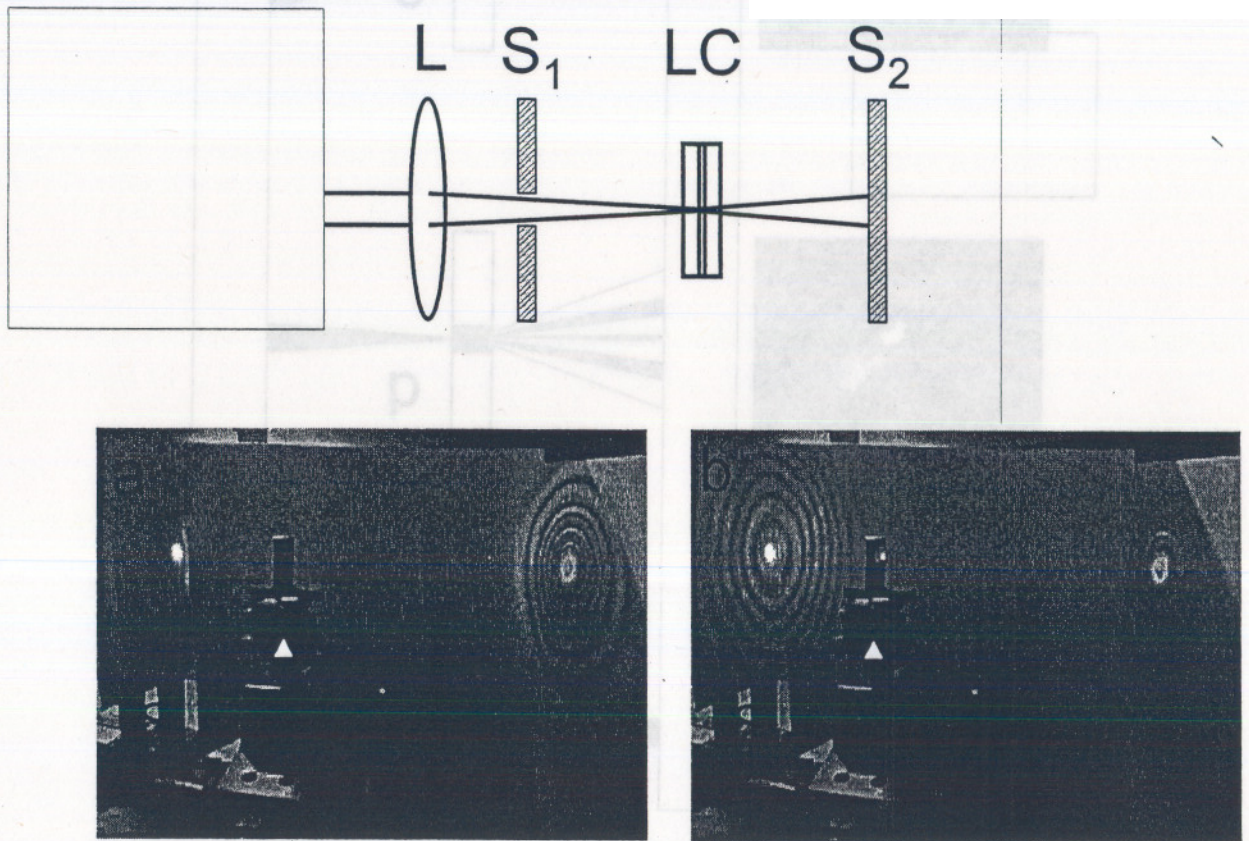

Fig. 9

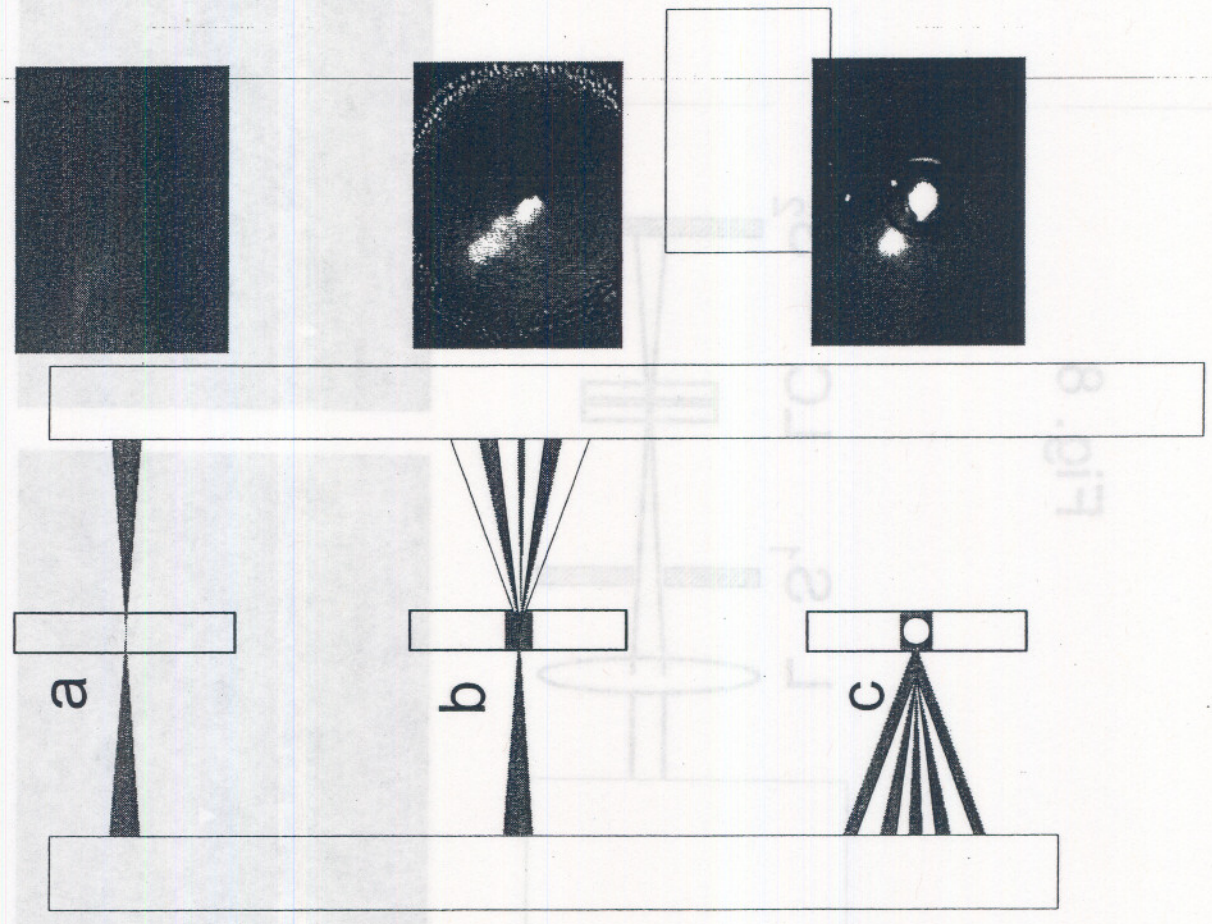

Fig. 10

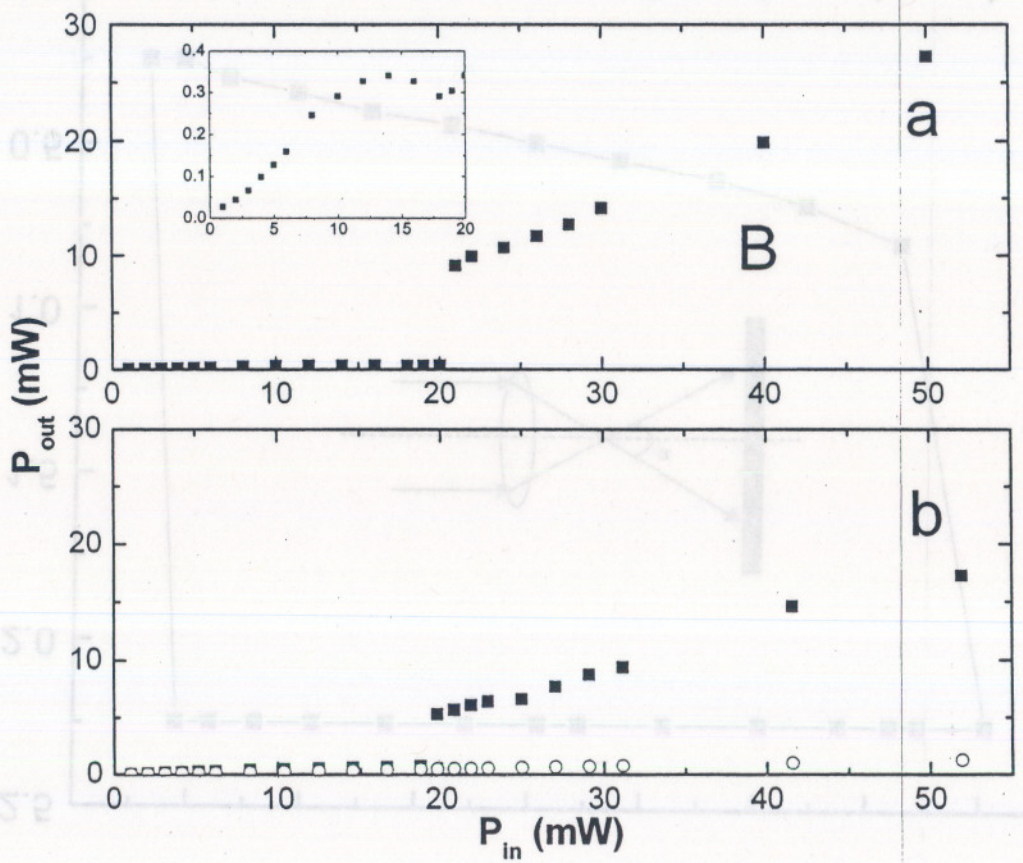

Fig. 11

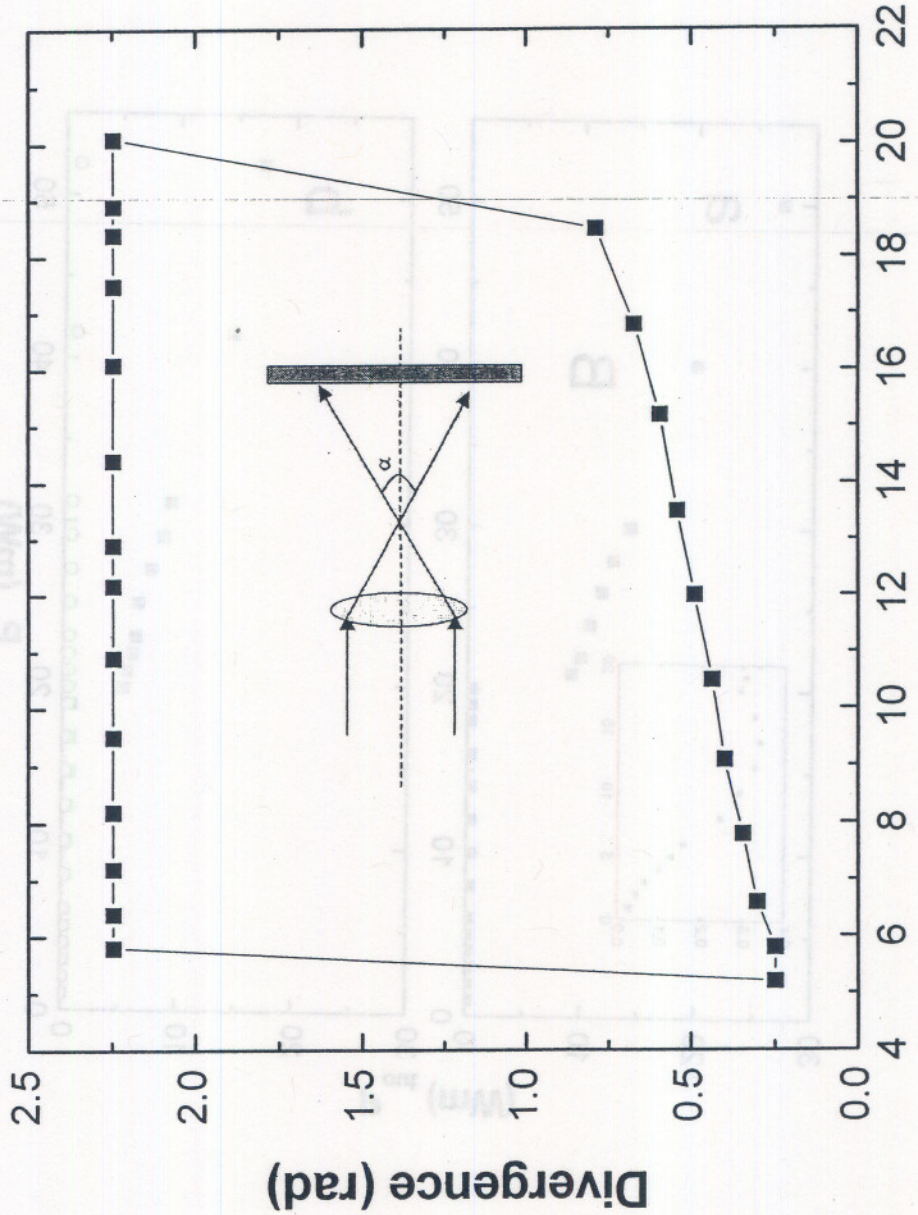
Divergence (rad)
Input Power (mW)
2.5
2.0
1.5
1.0
0.5
0.0
4
6
8
10
12
14
16
18
20
22
α